We are Nitinol.™

Effect of Wear and Crevice on the Corrosion Resistance of Overlapped Stents

Trepanier, Gong, Ditter, Pelton, Neely, Grishaber

Proceedings of the International Conference on Shape Memory and Superelastic Technologies, SMST-2006

2006

Proceedings of the International Conference on Shape Memory and Superelastic Technologies
May 7–11, 2006, Pacific Grove, California, USA
Brian Berg, M.R. Mitchell, and Jim Proft, editors, p 265-276
Copyright © 2008 ASM International®
All rights reserved.
DOI: 10.1361/cp2006smst265

Effect of Wear and Crevice on the Corrosion Resistance of Overlapped Stents

Christine Trépanier, Xiao-Yan Gong, Tom Ditter, and Alan Pelton
Nitinol Devices & Components, Fremont, California, USA

Yasmin Neely and Randy Grishaber
Cordis Corporation, Warren, New Jersey, USA

Abstract

This study assessed the effect of wear damage and crevice corrosion on Nitinol and stainless steel stents. Wear between the Nitinol or stainless steel stents was generated through *in vitro* axial fatigue tests of overlapped stents. SEM investigation of the stents after the fatigue test characterized the extent of wear damage on both Nitinol and stainless steel stents. Potentiodynamic polarization tests based on ASTM F2129 showed that both Nitinol and stainless steel are characterized by a decrease in the breakdown potential from about 900 mV vs SCE pre-fatigue test to about 550-650 mV vs SCE post-fatigue test. These results indicate that both groups of material are affected similarly by wear damage. In a separate study, potentiostatic polarization testing (ASTM F746) was used to evaluate the effect of crevice corrosion created by gaps between two overlapping Nitinol or stainless steel stents. The results from this study showed that both materials were able to repassivate crevice corrosion damage at 800 mV vs SCE.

Introduction

Most stent materials such as Nitinol and stainless steel rely on specific passivation treatments to form a passive thin surface oxide film (titanium or chromium oxide) to protect the base material from biocorrosion. Standard manufacturing processes for implant stents usually ends with surface passivation treatments such as electropolishing to reinforce this passive barrier against corrosion to optimize the biocompatibility of the material. However, implantation of multiple overlapping stents, which is a common procedure used in the treatment of long vascular lesions, such as in the Superior Femoral Artery (SFA), may lead to local damage or even removal of the passive film. This damage to the protective layer may decrease the resistance to localized corrosion (pitting), increase the corrosion rate, and possibly lead to increase ion release from the stents. Furthermore, implantation of multiple overlapping stents creates gaps between the two stents that may lead to crevice corrosion, which may also lead to a deterioration of the corrosion resistance. Although corrosion resistance of stainless steel and Nitinol has already been demonstrated in several studies [1-3], most studies were performed on single component and did not address the effect of wear damage and crevice that could possibly arise *in vivo*. Therefore, the goals of this study are to assess the effect of wear damage and crevice corrosion on Nitinol and stainless steel stents. Wear between the stents was first generated through *in vitro* fatigue tests of overlapped stents. The extent of wear was investigated with observations of the fretted surfaces and potentiodynamic polarization of the stents after fatigue testing while susceptibility to crevice corrosion was evaluated by potentiostatic polarization of overlapped stents.

Materials and Method

Prototype Nitinol stents (8 mm diameter X 25 mm long) Nitinol Devices & Components, Fremont, CA) and stainless steel stents (3.75 mm expanded diameter X 18 mm long) Cordis Corp., Warren, NJ) were used in this study. The stents were manufactured according to standard manufacturing practices for implant stents and were electropolished as a final passivation treatment.

Baseline corrosion resistance

The baseline corrosion resistance of each stent was established by performing potentiodynamic polarization of the stent in accordance with ASTM F2129 [4] in Hank's solution (Sigma Aldrich). The corrosion resistance of the specimens was characterized by the rest potential (E_r), the zero current potential (E_{zc}) and the breakdown potential (E_b). Reversal of the voltage scan after the breakdown was not performed to limit the damage to the stents.

Effect of crevice on the corrosion resistance

Potentiostatic polarization, in accordance with ASTM F746 [5], of overlapped stents at pre-selected potentials was used to assess the susceptibility to crevice corrosion of each stent. For this study, crevices were created by fully overlapping two Nitinol stents or two stainless steel stents prior to testing. After de-aeration of the solution for 30 min and monitoring of E_r for 1 hour, the stents were polarized to 800 mV vs SCE to stimulate localized crevice corrosion. The resultant current density was monitored as a function of time for a period of 15 min unless crevice corrosion was initiated. The various potentiostatic holds were determined from the potentiodynamic polarization curves obtained in the first part of this study. The potentiostatic holds for the Nitinol stents ranged from –350 mV up to 800 mV vs SCE. The potentiostatic holds for stainless steel stents ranged from –50 mV up to 800 mV vs SCE. For these tests, an asymptotically decreasing current density trend indicates that the material is able to repassivate localized corrosion. In contrast, an increasing current density trend indicates that localized corrosion (crevice corrosion) has been stimulated. The critical potential for pitting was reported as the most noble preselected potential at which the stents were able to repassivate after the stimulation step.

Effect of wear damage on the corrosion resistance

The effect of wear damage on the corrosion resistance of the material was assessed by performing potentiodynamic polarization test of stents that had been subjected to overlap axial fatigue tests prior to corrosion testing. The axial fatigue testing was chosen for two reasons. First, cyclic axial deformation is one of the most likely fracture modes in SFA due to walking. Second, it's highly likely that axial deformation is a more severe mode of deformation than pulsatile or crush deformation. Hence, we consider this deformation mode as a worst-case condition. The fatigue testing was performed on overlapped either Nitinol or stainless steel stents using a Bose Corporation LM1 TestBench-ELF Series tester. For each material, three pairs of overlapped stents were deployed in 5-7% radially compliant latex tubing (Dynatek Dalta, Inc.) with about half the length of the stent being overlapped. The overlapped stents were axially cycled with a mean displacement of 0.15mm and displacement amplitude of 0.15mm for 10 million cycles. Because mechanical properties of Nitinol are affected by temperature, fatigue testing of the overlapped Nitinol stents was performed at 37^{o}C in phosphate buffered saline solution (Amresco). For simplicity reasons and because stainless steel mechanical properties are not affected by a small temperature difference, fatigue testing of the overlapped stainless steel stents was performed at room temperature in phosphate buffered saline solution. After fatigue testing, wear damage was determined by optical microscopy and SEM. The corrosion resistance of each stent was then assessed individually by performing potentiodynamic polarization tests of the samples.

In accordance with ASTM F2129 and F746, an EG&G Princeton Applied Research potentiostat model 273A was used to conduct the corrosion tests. The potentiostat is controlled by a computer with PowerCORR software from AMETEK/PAR. A saturated calomel electrode (SCE) is used as a reference electrode for the potential. Two platinum auxiliary electrodes are used as counter electrodes. Testing was conducted in an appropriate polarization cell. The Hank's (H6136, Sigma Aldrich) solution was first de-aerated with nitrogen gas for 30 minutes prior to immersion of the test sample and throughout the test. Then, the Rest Potential (E_r) was monitored for one hour.

For the potentiodynamic polarization experiments (ASTM F2129), the polarization of the test specimen was then started 100 mV vs SCE below E_r at a voltage scan rate of 0.167 mV/sec. Unless otherwise specified, three sample pairs were tested for each material and condition. The samples were inspected with an optical microscope (10-60X) or scanning electron microscope (SEM, JEOL JSM 5600) after testing.

Results

Baseline corrosion resistance
Both Nitinol and stainless steel stents were characterized by a similar baseline corrosion resistance. All stents exhibited a stable corrosion behavior and passive region and reached the oxygen evolution potential (around 900 mV vs SCE). No evidence of localized corrosion (pitting) was observed on the stents post-corrosion testing. Typical polarization curves for each stent and a summary of the test results are presented in Fig. 1 and Table 1.

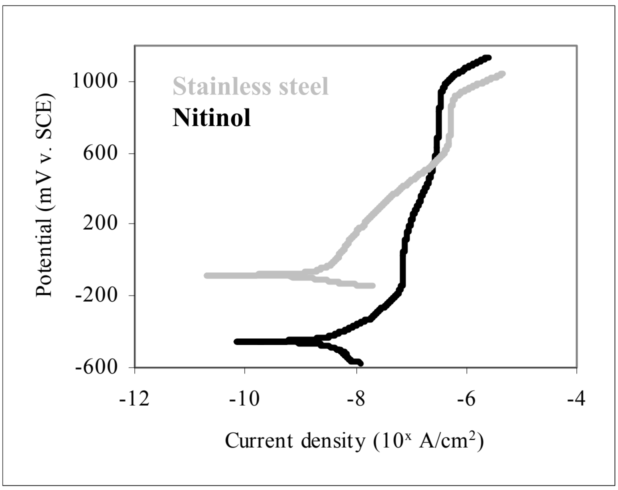

Figure 1: Typical polarization curves for stainless steel and Nitinol stents (baseline)

Table 1: Summary of baseline corrosion test results

Stent Material	E_r (mV vs SCE)	E_{zc} (mV vs SCE)	E_b (mV vs SCE)
NiTi	-402± 94	-402±63	937±24
SS	-40±8	-89±12	891±31

Effect of crevice on the corrosion resistance

Upon polarization to 800 mV, both groups of samples showed an increase in current density indicating the stimulation of localized crevice corrosion (see Fig. 2 for an example of initiation of localized corrosion). After cycling of the potential to lower values, both groups were able to repassivate the localized corrosion once they were re-polarized to 800 mV vs SCE (see Fig. 3 for an example of repassivation). A summary of the test results for each group of stents is presented in Table 2 and 3.

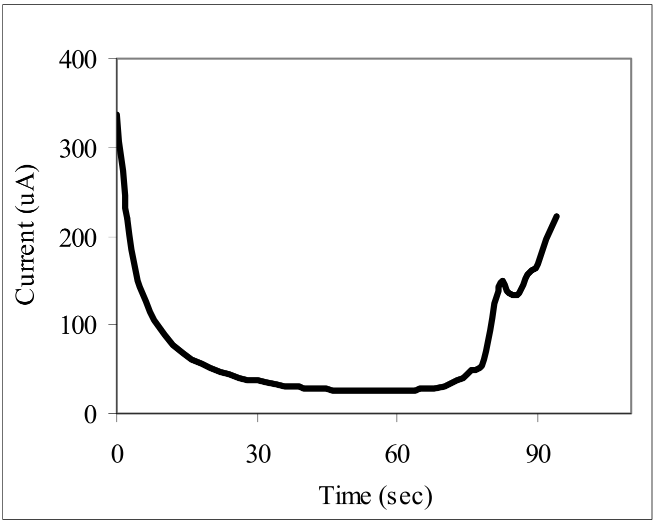

Figure 2:Typical curve showing an increase in current density during the potentiostatic hold indicating initiation of localized corrosion.

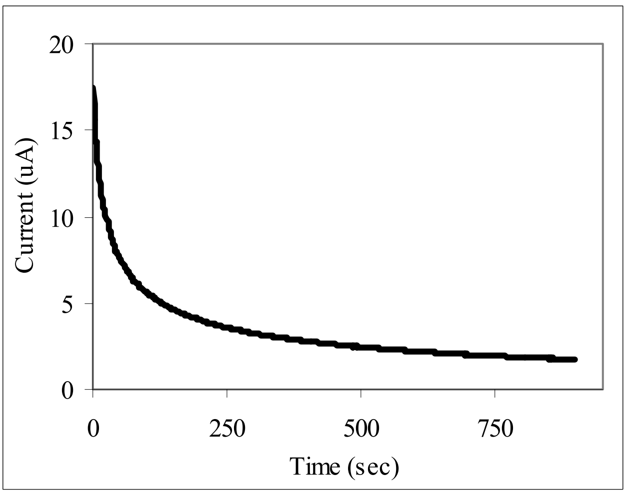

Figure 3: Typical curve showing a decrease in current density during the potentiostatic hold indicative of repassivation

*Table 2: Potentiostatic holds at different potentials for overlapped NiTi stents**

Stent #	800 mV vs SCE	-350 mV vs SCE	800 mV vs SCE	-250 mV vs SCE	800 mV vs SCE	-150 mV vs SCE	800 mV vs SCE
1-2	> I	R	> I	R	R		
3-4	> I	R	> I	R	> I	R	R
5-6	> I	R	R				

* > I indicates an increase in current and localized corrosion
R indicates a decrease in current and repassivation

*Table 3: Potentiostatic holds at different potential for overlapped stainless steel stents**

Stent #	800 mV vs SCE	-50 mV vs SCE	800 mV vs SCE	0 mV vs SCE	800 mV vs SCE
1-2	> I	R	R		
3-4	> I	R	R		
5-6	> I	R	> I	R	R

* > I indicates an increase in current and localized corrosion
R indicates a decrease in current and repassivation

Visual inspection of the stents after the corrosion test confirmed the presence of localized corrosion near overlapping stent struts (refer to Fig. 4 and 5) confirming the initiation of localized crevice corrosion during the test.

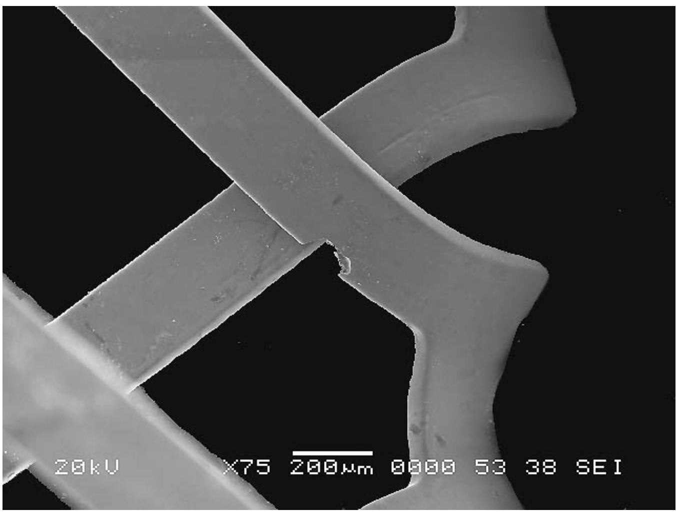

Figure 4: Initiation of localized corrosion at the intersection of two Nitinol stent struts

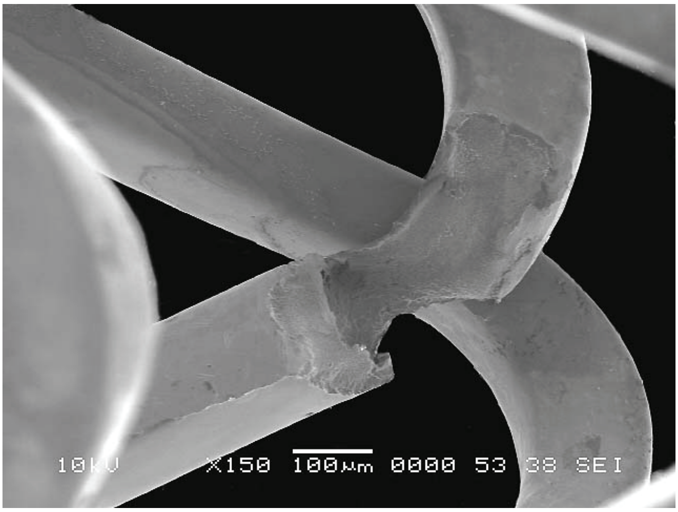

Figure 5: Initiation of localized corrosion at the intersection of two stainless steel stent struts

Effect of wear damage on the corrosion resistance
Evidence of wear damage was visible on all stents after the overlap axial fatigue test. Examples of wear damage observed on Nitinol and stainless steel stents is shown in Fig. 6 and 7. Clearly the "footprint" on Fig. 6 confirms the axial motion of 0.3mm was transferred to the micro motions on Nitinol stents. The stainless stent, however, did not show the clear micro motions between the struts, rather due to the small dimensions of the struts, they cut into each other and provided the severe damage on the struts as shown in Fig. 7. This observation indicates that fretting between struts depends upon the stent design and material.

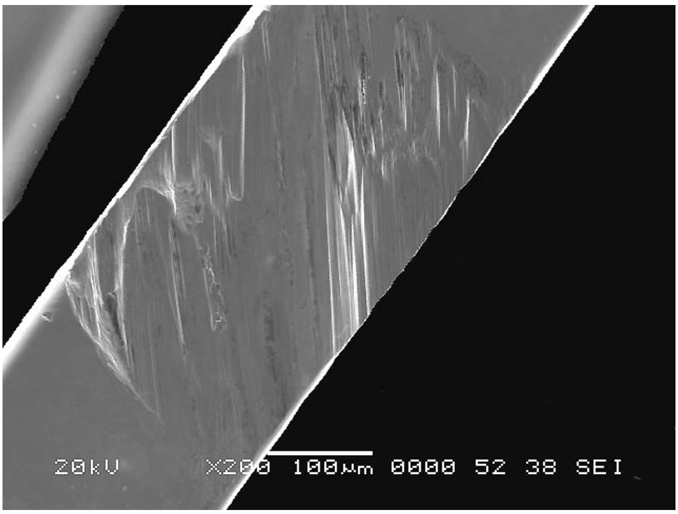

Figure 6: Wear damage on Nitinol stents after 10 million cycles axial fatigue testing (worst case).

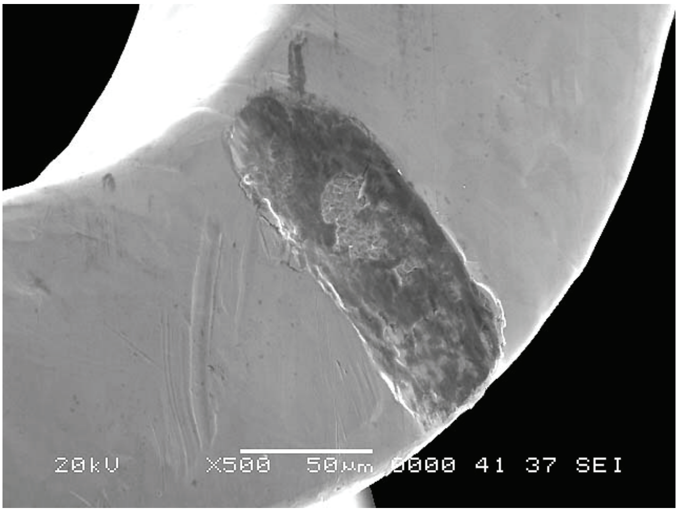

Figure 7: Wear damage on stainless steel stents after 10 million cycles axial fatigue testing (worst case).

The corrosion resistance of stents subjected to overlapped 10 million cycles axial fatigue is shown in Fig. 8 and is summarized in Table 4.

Post-fatigue tests, both groups of stents were characterized by a stable corrosion behavior. All stents exhibited localized corrosion during the tests. Both group of stents were characterized by a similar breakdown potential; the average breakdown potential for the Nitinol stents was 657 mV vs SCE while it was 554 mV vs SCE for the stainless steel stents (compared with 937 and 891 mV vs SCE respectively pre-fatigue testing).

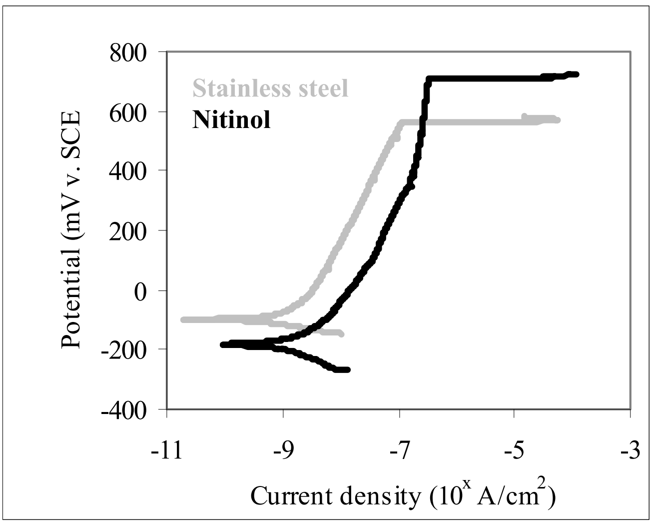

Figure 8: Potentiodynamic polarization curves of Nitinol and stainless steel stents post-fatigue testing.

Table 4: Summary of post-fatigue corrosion test results

Stent Material	E_r (mV vs SCE)	E_{zc} (mV vs SCE)	E_b (mV vs SCE)
NiTi	-227± 105	-257±115	657±171
SS	-86±24	-149±31	554±62

SEM investigation of the stents after corrosion testing revealed that in most cases, pitting did occur on the damaged surface area of the stent struts for both group of stents as shown in Figures 9 and 10.

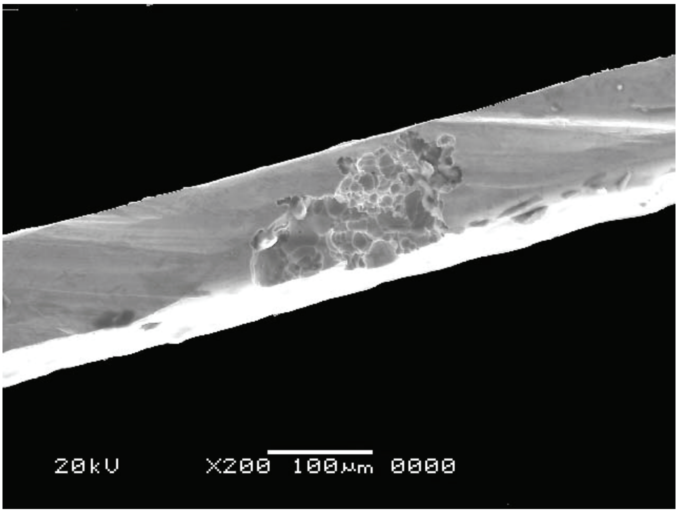

Figure 9: Evidence of localized corrosion (pitting) on the wear damaged area of a Nitinol stent.

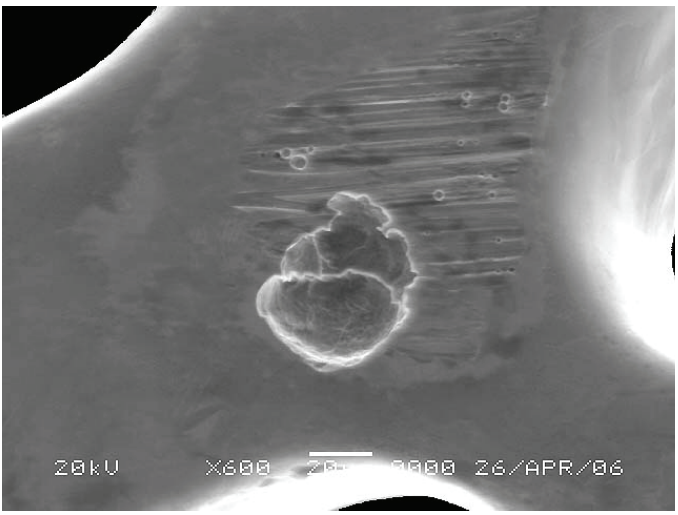

Figure 10: SEM micrograph of pit initiation site of wear damaged area of a stainless steel stent.

Discussion

This study showed that Nitinol and stainless steel stents can be susceptible to crevice corrosion when multiple stents are overlapped. However, the results of this study also showed the good capability of the materials to repassivate localized crevice corrosion once it has been initiated. These results are in good agreement with previous studies that demonstrate the good repassivation of these materials. Specifically, those studies show a small potential reversal hysteresis after breakdown [2, 7].

Axial fatigue testing of overlapped stents showed wear damage generated between the two surfaces as a result of the micromotion of both components on one another. SEM investigation post-fatigue testing revealed disruption of the oxide layer and formation of clear "footprints" on the stent surfaces. Previous studies have shown that the oxide layer thickness on electropolished Nitinol, similar to electropolished stainless steel, is on the order of 50-100Å [8-9]. Based on the SEM evaluation of the surface, it is most probable that the electropolished passive layer was fully worn away during the test and replaced by another oxide on the surface of the materials. The decrease in breakdown potential after wear indicates that the newly formed oxide layer is different from the original surface formed by electropolishing. In a previous study published by Thierry *et al*, the breakdown potential of mechanically polished Nitinol and stainless steel discs was similar to the breakdown potential of the stent post-fatigue testing obtained in our study [10]. This result suggests that the native oxide layer may be similar to the oxide layer found on mechanically polished specimens. Still, these stents perform similarly to predicate reference stainless steel Cordis Palmaz stents tested under similar conditions and, which exhibit excellent corrosion resistance and biocompatibility *in vivo* [3]. Therefore, this result suggests that, although the corrosion resistance of the prototype stents decreased after overlapped fatigue, they should still exhibit sufficient corrosion resistance *in vivo*.

Similar results were obtained in a previous study where passivated Nitinol and stainless steel discs underwent scratch damage using a diamond stylus. Results from potentiostatic polarization tests demonstrated good repassivation capability of both materials after their passive oxide layer had been disrupted [11].

It is important to note that the initial surface treatment of the stent surface played a key role in the stents good corrosion behavior. This is due to the fact that both these stents were passivated prior to fatigue testing to dissolve most of the heavy oxide and intermetallic phases. These heavy oxide and intermetallic phases were therefore not present on the surface of the material even when the thin electropolished layer was disrupted. As demonstrated in other studies, thermal oxidation of Nitinol leads to the formation of a mixture of Ni_3Ti, Ni and titanium oxide, which are covered by a titanium oxide outer layer [8, 9]. Although thermally oxidized Nitinol can have acceptable corrosion performance when the titanium oxide outer layer is intact [12-14], it has been shown that when subjected to small strain this oxide layer may crack and expose the nickel-rich phase beneath the passive layer and lead to unacceptable corrosion behavior [15]. The extent of the wear damage demonstrated in this study further demonstrate that a thick titanium oxide layer may be worn away when multiple stents are overlapped and lead to similar unacceptable corrosion resistance.

On the other hand, it is also important to note that our *in vitro* fatigue testing which was performed in an simulated physiological solution could not take into account the effect of cells, proteins and implant endothelialization that normally occurs *in vivo*. These biological elements may also play a role in the extent of wear damage that can occur *in vivo* and may affect corrosion resistance.

The results from this study warrant further investigation of the combined effects of crevice and wear corrosion on the stents. Further studies should also consider the effect of overlapping multiple stents of dissimilar materials, which adds a galvanic corrosion component to the effect observed in this paper. A more fundamental approach of the investigation of the real-time effect of wear corrosion by monitoring of the potential and/or current during the mechanical fatigue test should give important information of the loss of passivation and repassivation of the materials. Investigation of weight loss and/or ion release during the fatigue test may offer more information on the wear mechanisms of both materials. Finally, characterization of the nature and composition of the oxide layer that forms on Nitinol or stainless steel after wear should also be performed to better understand the oxidation mechanism at body temperature.

Conclusions

This study investigated the effect of wear and crevice corrosion of Nitinol and stainless steel stents. Wear between the stents was first generated through *in vitro* fatigue tests of overlapped stents. The extent of wear was investigated with observations of the fretted surfaces and potentiodynamic polarization of the stents after wear while susceptibility to crevice corrosion was evaluated by potentiostatic polarization of overlapped stents. The results from our study show:

- Both Nitinol and stainless steel stents are susceptible to crevice corrosion. During potentiodynamic polarization tests, both materials were able to repassivate localized crevice corrosion at 800 mV vs SCE.

- Both Nitinol and stainless steel stents are susceptible to wear damage during fatigue testing of overlapped stents.

- Potentiodynamic polarization testing reveals that the breakdown potential of both groups of stents decreases from an average of 900 mV vs SCE (oxygen evolution) down to an average of 550-650 mV vs SCE.

Based on these results it is concluded that under the current test conditions, Nitinol and stainless steel are characterized by similar corrosion resistance to wear damage and crevice corrosion that can occur when multiple stents are overlapped.

References

[1] Wiskirchen, J, Venugopalan, R. *et al.* "Radiopaque Marquers in Endovascular Stents – Benefits and Potential Hazards", *Fortschr Rontgenstr*, 175 (2003), pp. 484-488.
[2] Venugopalan, R., Trepanier, C., "Assessing the Corrosion Behaviour of Nitinol for Minimally-Invasive Device Design", *Min Invas Ther & Allied Technol*, 9, 2 (2000), pp. 67-74.
[3] Stoeckel, D., Pelton, A., Duerig, T., "Self-Expanding Nitinol Stents – Material and Design Considerations", European Radiology, Vol. 14, No. 2 (20030, pp.292-301.
[4] F2129, "Standard Test Method for Conducting Cyclic Potentiodynamic Polarization Measurements to Determine the Corrosion Susceptibility of Small Implant Devices", Annual Books of ASTM Standards, Medical Devices and Services, vol. 13.01, 2004.
[5] F746, "Standard Test Method for Pitting or Crevice Corrosion of metallic Surgical Implant Materials", Annual Books of ASTM Standards, Medical Devices and Services, vol. 13.01, 2004.

[6] Silva, M. et al "Average Patient Walking Activity Approaches Two Million Cycles per Year" *J. Arthroplasty*, Vol. 17, No. 6 (2002), pp. 693-697.

[7] Trepanier, C., Pelton, A.R., "Effect of Strain on the Corrosion Resistance of Nitinol and Stainless Steel in Simulated Physiological Environment", SMST-2003 Proceedings of the International Conference on Shape memory and Superelastic Technologies, SMST Society, Inc., (California, 2004), pp. 393-398.

[8] Trepanier, C., Tabrizian, M., Yahia, L'H., Bilodeau, L., Piron, D.L., "Effect of the Modification of the Oxide Layer on NiTi Stent Corrosion Resistance", *J Biomed Mater Res (Appl Biomater)*, 43 (1998), pp. 433-440.

[9] Zhu, L., Fino, J.M., Pelton, A.R., "Oxidation of Nitinol", SMST-2003 Proceedings of the International Conference on Shape memory and Superelastic Technologies, SMST Society, Inc., (California, 2004), pp. 357-366.

[10] Thierry, B., Tabrizian, M., Trepanier, C., Savadogo, O., Yahia, L'H., "Effect of Surface Treatment and Sterilization Processes on the Corrosion Behavior of NiTi Shape Memory Alloy", *J Biomed Mater Res*, 51 (2000), pp. 685-693.

[11] Trepanier, C., Venugopalan, R., Pelton, A.R., "Corrosion Resistance and Biocompatibility of Passivated NiTi", Shape Memory Implants, Springer (2000), pp. 35-45.

[12] Firstov, G.S., Vitchev, R.G., Kumar, H., Blanpain, B., Van Humbeecck, J., "Surface Oxidation of NiTi Shape memory Alloy", *Biomaterials*, 23 (2002), pp. 4863-4871.

[13] O"Brien, B., Carroll, W.M., Kelly, M.J., "Passivation of Nitinol Wire for Vascular Implants – A Demonstration of the Benefits", *Biomaterials*, 23 (2002), pp. 1739-1748.

[14] Barison, S., Cattarin, S., Daolio, S., Musiani, M., Tuissi, A., "Characterization of Surface Oxidation of Nickel-Tiatnium Alloy by Ion-Beam and Electrochemical Techniques", *Electrochemica Acta*, 50 (2004), pp.11-18.

[15] Trepanier, C., Zhu, L., Fino, J., Pelton, A.R., "Corrosion Resistance of Oxidized Nitinol", SMST-2003 Proceedings of the International Conference on Shape memory and Superelastic Technologies, SMST Society, Inc., (California, 2004), pp. 367-373.